Rhoptry neck protein 11 has crucial roles during malaria parasite sporozoite invasion of salivary glands and hepatocytes

Sirasate Bantuchai [a], Mamoru Nozaki [b,1], Amporn Thongkukiatkul [c], Natcha Lorsuwannarat [a,2], Mayumi Tachibana [a,b], Minami Baba [a,b], Kazuhiro Matsuoka [a,b,3], Takafumi Tsuboi [d], Motomi Torii [a,b], Tomoko Ishino [a,b,*]

[a] Department of Molecular Parasitology, Graduate School of Medicine, Ehime University, Toon, Ehime 791-0295, Japan
[b] Division of Molecular Parasitology, Proteo-Science Center, Ehime University, Toon, Ehime 791-0295, Japan
[c] Department of Biology, Faculty of Science, Burapha University, Chonburi 20131, Thailand
[d] Division of Malaria Research, Proteo-Science Center, Ehime University, Matsuyama, Ehime 790-8577, Japan

ABSTRACT

The malaria parasite sporozoite sequentially invades mosquito salivary glands and mammalian hepatocytes; and is the *Plasmodium* lifecycle infective form mediating parasite transmission by the mosquito vector. The identification of several sporozoite-specific secretory proteins involved in invasion has revealed that sporozoite motility and specific recognition of target cells are crucial for transmission. It has also been demonstrated that some components of the invasion machinery are conserved between erythrocytic asexual and transmission stage parasites. The application of a sporozoite stage-specific gene knockdown system in the rodent malaria parasite, *Plasmodium berghei*, enables us to investigate the roles of such proteins previously intractable to study due to their essentiality for asexual intraerythrocytic stage development, the stage at which transgenic parasites are derived. Here, we focused on the rhoptry neck protein 11 (RON11) that contains multiple transmembrane domains and putative calcium-binding EF-hand domains. *Pb*RON11 is localised to rhoptry organelles in both merozoites and sporozoites. To repress *Pb*RON11 expression exclusively in sporozoites, we produced transgenic parasites using a promoter-swapping strategy. *Pb*RON11-repressed sporozoites showed significant reduction in attachment and motility in vitro, and consequently failed to efficiently invade salivary glands. *Pb*RON11 was also determined to be essential for sporozoite infection of the liver, the first step during transmission to the vertebrate host. RON11 is demonstrated to be crucial for sporozoite invasion of both target host cells – mosquito salivary glands and mammalian hepatocytes – via involvement in sporozoite motility.

© 2019 The Author(s). Published by Elsevier Ltd on behalf of Australian Society for Parasitology. This is an open access article under the CC BY-NC-ND license (http://creativecommons.org/licenses/by-nc-nd/4.0/).

1. Introduction

Plasmodium, the causative agent of malaria, has a complex life-cycle that requires switching between a vertebrate host and mosquito vector, and transmission from the latter is mediated by sporozoites. Sporozoites develop within oocysts on the basal lamina of mosquito midguts, and then invade salivary glands following their release from oocysts into the haemocoel. During a blood meal, sporozoites are injected into the mammalian host skin, through which they actively migrate to enter blood vessels, and eventually reach the liver to initiate infection of hepatocytes. Therefore, invasion of salivary glands in mosquito vectors and invasion of hepatocytes in mammalian hosts are key steps for *Plasmodium* sporozoites to achieve effective transmission.

The application of reverse genetic approaches has identified several sporozoite proteins as important molecules for parasite transmission (reviewed in Aly et al., 2009). For example, targeted gene disruption of sporozoite surface proteins showed that sporozoite motility is essential not only for migration but also for invasion capacity (Sultan et al., 1997; Menard, 2001; Vanderberg and Frevert, 2004; Combe et al., 2009; Steinbuechel and Matuschewski, 2009; Ejigiri et al., 2012). Sporozoites activated by incubation in albumin-containing medium, mimicking the

* Corresponding author at: Division of Molecular Parasitology, Proteo-Science Center, Ehime University, Toon, Ehime 791-0295, Japan. Fax: +81 89 960 5287.
E-mail address: tishino@m.ehime-u.ac.jp (T. Ishino).
[1] Present address: Toyama Prefectural University, Graduate School of Engineering, Plant and Cell Engineering Lab. 5180 Kurokawa, Imizu-shi, Toyama 939-0398, Japan.
[2] Present address: Department of Anatomy, Phramongkutklao College of Medicine, Rajavithi Road, Bangkok 10400, Thailand.
[3] Present address: Clinical Research Center, National Hospital Organization Nagoya Medical Center, Nagoya, Aichi 460-0001, Japan.

environment of mammalian skin, start circular locomotion on glass slides, termed gliding motility. Thrombospondin-related adhesive protein (TRAP) is a key molecule in *Plasmodium* sporozoite gliding motility, and links extracellular substrate adhesion with an intracellular actomyosin motor complex via a single transmembrane domain (Sultan et al., 1997; Kappe et al., 1999; Matuschewski et al., 2002). TRAP mediated recognition of salivary glands might be in part via interaction with a salivary gland surface protein, SAGLIN (Ghosh et al., 2009). Membrane-associated erythrocyte binding-like protein (MAEBL) is another essential molecule for salivary gland invasion, presumably by acting as an adhesin (Kariu et al., 2002; Saenz et al., 2008; Yang et al., 2017). Most of the known invasion related proteins in sporozoites are stored in apical secretory organelles termed micronemes, which are conserved among the invasive stages of apicomplexan parasites (Sibley et al., 2010). Discharge of TRAP from micronemes during sporozoite motility and invasion was demonstrated to be initiated by increasing intracellular Ca^{2+}, stimulated by activation mimicking environmental triggers in mammalian skin, and enhanced by sporozoite attachment to substrates (Carey et al., 2014).

Infective stages of apicomplexan parasites, such as *Plasmodium* merozoites, sporozoites, and *Toxoplasma* tachyzoites, have another distinct apical organelle, termed the rhoptry, which contains secretory proteins required for target cell invasion (Bradley and Sibley, 2007). It has been demonstrated that some rhoptry proteins have common roles during target cell invasion of infective stage parasites. For example, rhoptry neck protein 2 (RON2) was demonstrated to be crucial for tight junction formation between parasites and host cells by insertion into the target cellular membrane prior to invasion, for both *Plasmodium* merozoites during invasion of red blood cells, and *Toxoplasma* tachyzoites, which can invade a variety of nucleated cells (Besteiro et al., 2009; Proellocks et al., 2010). Recently we applied a sporozoite stage-specific knockdown system to demonstrate that sporozoite RON2 in *Plasmodium berghei* (*Pb*) is crucial for invasion of mosquito salivary glands and important for infection of mammalian hepatocytes (Ishino et al., 2019). These results implicate that further investigations on sporozoite rhoptry proteins are needed to elucidate the comprehensive mechanisms of sporozoite invasion of host cells.

Rhoptry neck protein 11 (RON11) was first described as localised to the rhoptry neck in *Toxoplasma* tachyzoites (Beck et al., 2013). It has an architecture of seven transmembrane domains plus two putative calcium binding EF-hand domains, and is highly conserved in the Apicomplexa, suggesting an important role in rhoptry-mediated functions. Attempts to disrupt *Pb*RON11 (PBANKA_132710 in PlasmoDB) have failed (Lasonder et al., 2008; van Ooij et al., 2008), supporting that RON11 has a crucial role during blood stage parasite proliferation. Here, to investigate a role of RON11 in sporozoites, we generated sporozoite stage-specific *pbron11* knockdown parasites in *P. berghei* by promoter swapping (Ishino et al., 2019). *Pb*RON11-repressed sporozoites have decreased adhesion capacity to glass slides and motility in vitro, and greatly reduced invasion efficiency in mosquito salivary glands. In addition, *pbron11* repression in sporozoites results in a significant reduction in sporozoite infectivity to the mouse liver in vivo. These findings clearly demonstrate that *Pb*RON11 in sporozoites is essential for salivary gland invasion and mammalian liver infection due to its role in adhesion and gliding motility.

2. Materials and methods

2.1. Experimental animals

Female ICR and C57BL6 mice, and Wistar rats were purchased from CLEA Japan (Tokyo, Japan) and maintained in our animal facility. All mice were 6–8 weeks old at the time of blood stage parasite infection. Animal experimental protocols were approved by the Institutional Animal Care and Use Committee, Ehime University, Japan. All experiments were conducted according to the Ethical Guidelines for Animal Experiments of Ehime University.

2.2. Parasites and mosquitoes

Anopheles stephensi mosquitoes (SDA 500 strain) were reared using standard protocols (Sinden et al., 2002) and maintained on a 5% sucrose solution during adult stages. All parasites were derived from a *P. berghei* ANKA strain which expresses GFP under the control of the *elongation factor 1A* (*ef1α*) promoter without any drug-resistant cassette (*Pb*WT-GFP; Franke-Fayard et al., 2004), kindly provided by Dr. Janse, Leiden University, Netherlands. Cryopreserved *P. berghei*-infected erythrocytes were inoculated into 4–6 weeks old female ICR mice (CLEA Japan) via i.p. injection to obtain asexual stage parasites. Approximately 60,000 parasitised erythrocytes were transferred intravenously into a naïve mouse 5 days before mosquito feeding. When the parasitemia reached 5–10% and the number of exflagellation centres had reached 30 per 1×10^5 erythrocytes, the infected mice were fed on by a group of female mosquitoes. Fully engorged mosquitoes were selected and maintained at 20 °C.

2.3. Production of recombinant proteins and preparation of anti-PbRON11N antibodies and anti-TRAP ectodomain antibodies

To generate *Pb*RON11 polyclonal antibodies, a partial recombinant protein corresponding to amino acids 26–320 of *Pb*RON11 (*Pb*RON11N, indicated by a bar in Fig. 1A) was produced using the wheat germ cell-free protein synthesis system (CellFree Sciences, Matsuyama, Japan) as described (Tsuboi et al., 2008). Briefly, DNA encoding *Pb*RON11N was amplified by PCR from genomic DNA of *Pb* wild type (WT)-GFP using specific primers tailed with *Eco*RV and *Bam*HI restriction enzyme recognition sites (shown in Supplementary Table S1). The DNA fragment was inserted into the pEU-E01-GST-TEV-MCS vector (CellFree Science) to produce GST-tagged *Pb*RON11N at its N-terminal. After transcription and translation using the wheat germ cell-free protein expression system, recombinant protein was purified using a glutathione-Sepharose 4B column (GE Healthcare UK, Buckinghamshire, UK). For production of polyclonal antibodies recognising the TRAP ectodomain, a partial recombinant protein corresponding to amino acids 26–541 of *Pb*TRAP (PBANKA_1349800) was produced as described above.

A Japanese white rabbit was immunised subcutaneously with 250 µg of purified recombinant protein with Freund's adjuvant three times, and antisera was obtained 14 days after the final immunisation (Kitayama Labes, Ina, Japan). The reactivity and specificity of anti-*Pb*RON11N antisera was determined by western blotting. Specific antibodies against *Pb*RON11N were affinity purified using recombinant *Pb*RON11N protein covalently conjugated to HiTrap NHS-Activated HP columns (GE Healthcare, Oda-Yokouchi et al., 2019).

2.4. Schizont preparation

All procedures were performed as described in Janse et al. (2006) with some modification. Infected blood with 3–5% parasitemia was collected from 5-week-old Wistar rats and cultured in complete RPMI 1640 medium (Wako Pure Chemical, Osaka, Japan) containing 20% foetal calf serum (FCS) with a gas mixture of 5% CO_2, 5% O_2, and 90% N_2, for 16 h at 36.5 °C with slow agitation. Schizonts were purified using Nycoprep 1.077 solution (Axis-shield, Dundee, UK) by centrifugation at 450g for 20 min.
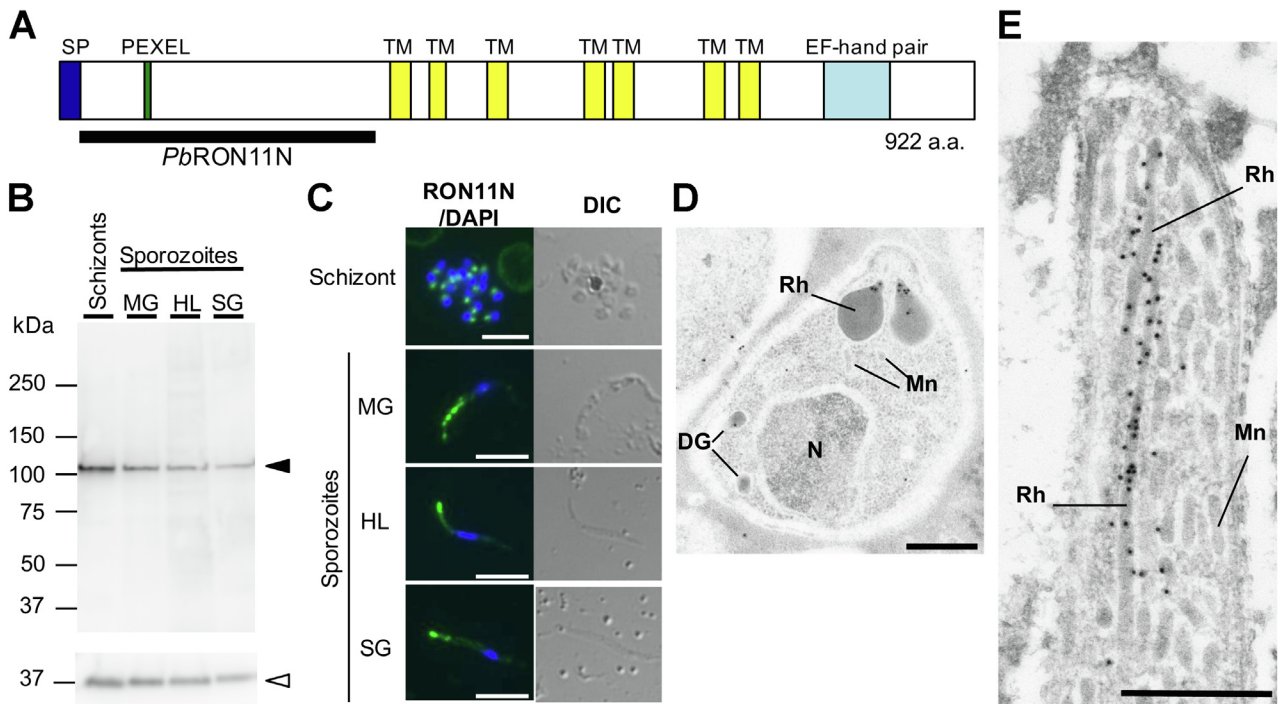
Fig. 1. Expression and localisation of rhoptry neck protein 11 (RON11) in *Plasmodium berghei* merozoites and sporozoites. (A) Schematic of protein features of *Pb*RON11. Signal peptide, PEXEL motif, transmembrane domains, and an EF-hand domain pair are indicated. The predicted molecular weight of *Pb*RON11 protein excluding a signal peptide is 108 kDa. A black bar indicates the region used in the production of *Pb*RON11N recombinant protein. (B) *Pb*RON11 protein expression in sporozoites collected from mosquito midguts (MG), haemolymph (HL), salivary glands (SG), and schizonts. Protein from parasite lysates corresponding to 10,000 schizonts and 100,000 sporozoites were separated by electrophoresis and western blotting was performed using anti-*Pb*RON11N antibodies. *Pb*RON11 protein was detected specifically at approximately 100 kDa both in schizonts and in sporozoites (closed arrowhead). The same membrane was stained with anti-rhoptry-associated membrane antigen (RAMA) antibodies as a loading control (indicated by an open arrowhead). *Pb*RAMA was processed and detected as a major band at approximately 37 kDa in sporozoites as well as in schizonts (Topolska et al., 2004). The quantification of RON11 band intensities normalised by RAMA is shown in Supplementary Fig. S4A. (C) *Pb*RON11 localisation at the apical end of infective stage parasites. IFA was performed with *Pb* wild type (WT)-GFP schizonts and sporozoites isolated from mosquito midguts, haemolymph, or salivary glands using anti-*Pb*RON11N antibodies. *Pb*RON11 signal (green (white)) and parasite nuclei (stained by DAPI, blue (grey)) are shown. Differential interference contrast images are shown. Scale bars = 5 μm. (D, E) Localisation of *Pb*RON11 in merozoites and sporozoites determined by immunoelectron microscope analysis. Ultrathin sections of (D) *Pb*WT-GFP schizonts or (E) salivary gland-derived *Pb*RON11-c-Myc sporozoites were incubated with anti-*Pb*RON11N or anti-c-Myc antibodies, respectively, followed by secondary antibodies conjugated to gold particles. N, nucleus; Rh, rhoptry; Mn, microneme; DG, dense granule; a.a., amino acid. Scale bars = 500 nm.

The schizont-rich layer was harvested and used for immunofluorescence analysis (IFA) and DNA transfection. For western blotting, schizont parasitised erythrocytes were treated with 0.08% saponin for 10 min prior to resuspension in SDS buffer (Nacalai tesque, Kyoto, Japan).

2.5. Sporozoite collection from infected mosquitoes

Oocyst-derived sporozoites were collected from infected mosquito midguts at days 23–24 post-feeding and then purified by 17% Accudenz density gradient centrifugation (Accurate Chemical, Westbury, NY, USA, Kennedy et al., 2012). Sporozoites released into the haemocoel were collected by perfusion with RPMI 1640 medium at days 22–23 post-feeding. Salivary gland sporozoites were collected by microdissection of salivary glands at days 23–24 post-feeding.

2.6. Western blotting

For *Pb*RON11 protein expression analysis, 10^4 schizonts, 10^5 oocyst-derived sporozoites, haemolymph sporozoites, and salivary gland sporozoites were resuspended in SDS buffer (Nacalai tesque) with the addition of 10% 2-mercaptoethanol and incubated at 4 °C overnight. *Pb*RON11 protein could not be detected in the following western blotting protocol if first denatured at 95 °C for 5 min, presumably due to aggregation. Proteins were separated on 12.5% e-PAGEL (ATTO, Tokyo, Japan) and transferred to polyvinylidene

difluoride (PVDF) membranes (Millipore, Burlington, VT, USA) by electroblotting. Membranes were blocked with Blocking One buffer (Nacalai tesque) and incubated with anti-*Pb*RON11N antibodies (1.46 μg/ml) at 4 °C overnight or at 37 °C for 1 h followed by incubation with anti-rabbit IgG antibodies conjugated with horse radish peroxidase (HRP) (1:25,000) at 37 °C for 45 min. Anti-rhoptry-associated membrane antigen (RAMA; PBANKA_0804500) antibodies (2.75 μg/ml) were used in parallel as an internal control (Ishino et al., 2019). Secondary antibody signals were developed using the Immobilon Western Chemiluminescent HRP Substrate (Millipore) and detected using the ImageQuant LAS4000 imaging system (GE Healthcare).

2.7. Immunofluorescence analysis (IFA)

Schizont-rich parasites were smeared on glass slides, then fixed with acetone for 2–5 min at 4 °C. Sporozoites isolated from midguts, haemocoel, and salivary glands of infected mosquitoes were spotted on glass slides and then fixed with acetone as described above. Slides were blocked with Blocking One Histo (Nacalai tesque) and incubated with anti-*Pb*RON11N antibodies (1.46 μg/ml). After washing with PBS, slides were incubated with fluorescent-conjugated secondary antibodies (Alexa Fluor 488 goat anti-rabbit IgG, 1:500; Thermo Fisher Scientific, Waltham, MA, USA) for 45 min at 37 °C. Stained slides were mounted with Prolong Gold anti-fade reagent containing DAPI (Thermo Fisher Scientific). Differential interference contrast (DIC) and fluorescence images

were obtained using a fluorescence microscope (Axio observer z1, Carl Zeiss, Oberkochen, Germany) and a charge-coupled device camera (Axio cam MR. Carl Zeiss). Images were processed using Image J software (Schneider et al., 2012).

2.8. Immunoelectron microscope (IEM)

Cultivated schizonts of PbWT-GFP and PbRON11-c-Myc expressing parasites (see below for generation of PbRON11-c-Myc expressing parasites) were fixed in 1% paraformaldehyde, 0.2% glutaraldehyde and embedded in LR-White resin (Polyscience, Warrington, PA, USA). Salivary glands of mosquitoes infected with PbWT-GFP and PbRON11-c-Myc expressing parasites were collected by dissection at day 19 post-feeding and fixed as described above. Ultrathin sections were blocked in PBS containing 5% non-fat milk and 0.01% Tween 20 (PBS-MT), then incubated at 4 °C overnight with anti-PbRON11N antibodies (72 µg/ml) or anti-c-Myc polyclonal antibodies (10 µg/ml) (A-14, sc-789; Santa Cruz Biotechnology, Dallas, TX, USA). The sections were washed with PBS containing 10% Block Ace (Yukijirushi, Tokyo, Japan) and 0.01% Tween 20 (PBS-BT), and the grids were incubated for 1 h at 37 °C with goat anti-rabbit IgG conjugated with 15 nm gold particles (GE Healthcare) diluted 1:20 in PBS-MT, and rinsed with PBS-BT. The sections were then stained with uranyl acetate and lead citrate. Samples were examined using a transmission electron microscope (JEM-1230; JEOL, Akishima, Japan).

2.9. Generation of transgenic parasites

To generate PbRON11-c-Myc expressing parasites, the pbron11 locus in PbWT-GFP parasites was replaced with an expression cassette in which RON11 is fused with a c-Myc tag at the C-terminus by single crossover homologous recombination (see Supplementary Fig. S1). To generate the transgenic vector, the pL0033 vector, obtained from BEI Resource (USA), was modified as follows. The partial coding region of PbRON11, 3217–4936 bp from the start codon, was amplified using primers as shown in Supplementary Table S1 and inserted into the pL0033 vector using SacII and NcoI restriction enzymes. This transgenic vector was linearised by StyI enzyme prior to transfection.

To produce sporozoite stage-specific pbron11 knockdown transgenic parasites (PbRON11-cKD), the 5′ untranslated region (UTR) of pbron11 was replaced by a promoter region of merozoite surface protein 9 (pbmsp9; PBANKA_1443300) using double crossover homologous recombination (see Fig. 2A; Ishino et al., 2019). Two homologous recombination cassettes, pbron11 upstream (−1829 to −996 bp relative to the PbRON11 start codon) and PbRON11-N (−24 to +893 bp), respectively, were sub-cloned into a vector containing the human dihydrofolate reductase (hDHFR) expression cassette, which was used for drug selection (Supplementary Fig. S2). The promoter region of pbmsp9 (−1253 to −3 bp) was inserted into the transgenic vector in front of the PbRON11N region and then the transfection vector was linearised by XhoI.

Transfection of the transgenic vector to PbWT-GFP schizonts was performed as described (Janse et al., 2006). Briefly, 10 µg of linearised PbRON11-c-Myc or PbRON11-cKD vector were transfected into schizont-enriched PbWT-GFP parasites by electroporation using Nucleofector (LONZA, Basel, Switzerland). The transgenic parasites were selected by adding 70 µg/ml of pyrimethamine to the drinking water after parasite inoculation into 4-week-old ICR female mice. The control parasites, PbRON11-cont, were generated using the same strategy except containing the pbron11 promoter region instead of the pbmsp9 promoter (see Fig. 2B and Supplementary Fig. S2). The sequences of all primers used in this study are listed in Supplementary Table S1. A clone of PbRON11-c-Myc expressing parasite, two clones of Pb-

RON11-cKD, and a clone of PbRON11-cont were isolated by limiting dilution.

2.10. Genomic Southern blot analysis

Genomic DNA was extracted from PbWT-GFP, PbRON11-cont, or PbRON11-cKD parasite-infected erythrocytes using a Wizard Genomic DNA purification kit (Promega, Madison, WI, USA). Ten micrograms of genomic DNA were digested with BamHI and XmnI restriction enzymes overnight, precipitated with 70% ethanol, and then electrophoretically separated in a 0.8% agarose gel. The DNA fragments were transferred to a Hybond-N+ membrane (GE-Healthcare) using the alkaline transfer method. To detect the integrated DNA locus, a probe corresponding to the hDHFR expression cassette region was amplified using specific primers (Supplementary Table S1) and labelled by alkaline phosphatase (AlkPhos Direct Labelling Module; GE Healthcare). After hybridisation at 55 °C overnight, excess probe was washed with preheated primary washing buffer (2 M urea, 0.1% SDS, 50 mM NaH_2PO_4 pH 7.0, 150 nM NaCl, 1 mM $MgCl_2$ and 0.2% w/v Blocking reagent; GE Healthcare) from the membrane. The signals were developed using CDP-star (CDP-Star Detection Reagent; GE Healthcare) and visualised using the ImageQuant LAS4000 imaging system (GE Healthcare).

2.11. Real-time reverse transcription (RT)-PCR

To confirm the reduction of pbron11 transcription in PbRON11-cKD sporozoites, real-time reverse transcription (RT)-PCR was carried out using specific primers as shown in Supplementary Table S1, as described in Ishino et al. (2019). Total RNA was extracted from 10-15 infected midguts at days 16–17 post-feeding using the RNeasy Micro Kit (Qiagen GmbH, Hilden, Germany). After DNase treatment, cDNA was synthesised using a PrimeScript RT reagent Kit (Perfect Real Time, Takara Bio, Otsu, Japan). Real time RT-PCR was performed using the TaKaRa PCR Thermal Cycler Dice with a SYBR Premix Ex Taq (Takara Bio) and pbron11-specific primers. A primer set for detection of heat shock protein-70 (hsp70; PBANKA_0711900), was used for normalisation (Acharya et al., 2007, Shonhai et al., 2007). Analysis of transcript levels relative to the average level of the internal control gene was calculated using the delta, delta-Ct method (Pfaffl, 2001). The experiment was performed four times using independently prepared samples from different infections, and the mean and standard deviations were determined.

2.12. Comparison of the numbers of sporozoites collected from mosquito bodies

Oocyst numbers of at least five mosquito midguts were counted at day 12 post-feeding to select mosquito groups with >60% prevalence for further experiments. At day 23 post-feeding, oocyst, haemolymph, and salivary gland-associated sporozoites were collected from 30 to 50 infected mosquitoes, and the sporozoite numbers were compared per mosquito. Experiments were repeated more than four times.

2.13. Analysis of sporozoite infectivity to mice

Twenty thousand haemolymph sporozoites collected on day 23 post-feeding were injected intravenously into 5-week old female C57BL/6 mice. Quantitative RT-PCR was performed as described by Ishino et al. (2019). Livers were perfused and collected at 24 h post inoculation and homogenised in 5 ml TRizol reagent (Thermo Fisher Scientific) using a Polytron PT1300D (Kinematica, Luzern, Switzerland). Total RNA was extracted using 1/25 vol of total
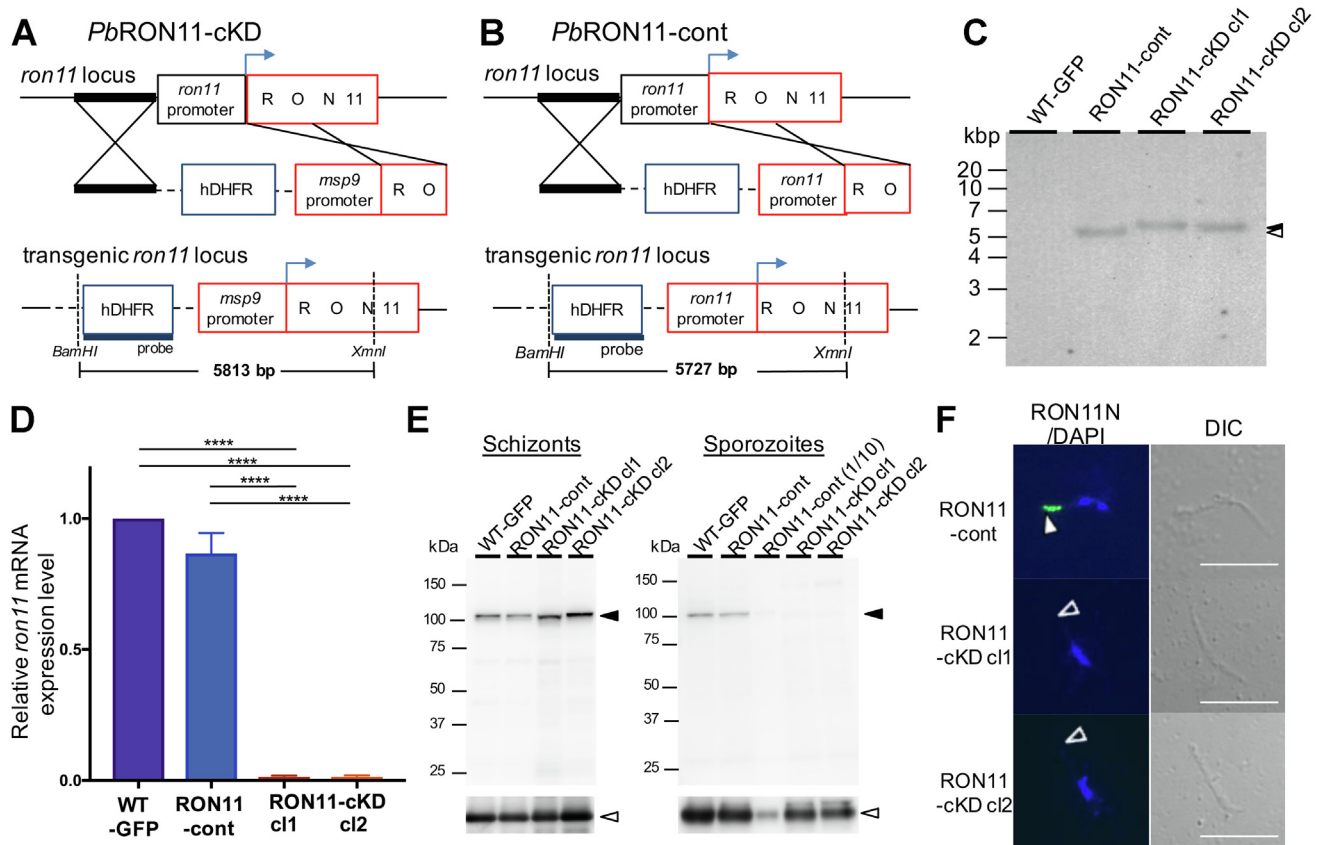
Fig. 2. Construction of sporozoite stage-specific *Plasmodium berghei* rhoptry neck protein 11 (*Pb*RON11) knockdown parasites. (A) Schematic of double-crossover homologous recombination to replace the *pbron11* promoter region with a *pb merozoite surface protein 9 (msp9)* promoter, to generate sporozoite stage-specific *pbron11* knockdown parasites (*Pb*RON11-cKD). A human dihydrofolate reductase expressing cassette (hDHFR) was designed for drug selection of transgenic parasites. The expected transgenic *ron11* locus after recombination is illustrated below, with the location of diagnostic restriction enzyme recognition sites and location of the probe used for Southern blotting (see Fig. 2C). (B) Schematic of the integrated locus for *Pb*RON11 control parasites (*Pb*RON11-cont). A similar DNA construct was used for integration into the *pbron11* locus as in (A), except containing a *pbron11* promoter region instead of the *pbmsp9* promoter. (C) Southern blot analysis to confirm correct DNA insertion into the *pbron11* locus. Genomic DNA of *Pb* wild type (WT)-GFP, *Pb*RON11-cont, or *Pb*RON11-cKD parasites was digested with *Bam*HI and *Xmn*I, separated by size via agarose gel electrophoresis, and transferred to a membrane. The specific signals were obtained by hybridisation of the DNA probe within the hDHFR cassettes at expected sizes indicated by an open and closed arrowhead for *Pb*RON11-cont and *Pb*RON11-cKD, respectively. (D) Bar graph representation of *pbron11* relative mRNA expression level in oocyst-derived sporozoites. Total RNA was extracted from mosquito midguts infected with *Pb*WT-GFP, *Pb*RON11-cont, *Pb*RON11-cKD cl1, or *Pb*RON11-cKD cl2 at day 17 post-feeding. The values were normalised by the expression of *pb heat shock protein 70 (hsp70)* mRNA in each sample. Experiments were repeated four times with independently prepared set of samples and the means with standard deviations were shown as bar graphs. Statistical differences were calculated by the one-way ANOVA with Tukey's multiple comparisons test ($^{****}P < 0.0001$). (E) Western blot analysis of *Pb*RON11 in schizonts and sporozoites. Protein homogenates of 10,000 schizonts and 100,000 or 10,000 oocyst-derived sporozoites of *Pb*WT-GFP, *Pb*RON11-cont, *Pb*RON11-cKD cl1, or *Pb*RON11-cKD cl2 were separated by SDS–PAGE and *Pb*RON11 was detected using anti-*Pb*RON11N antibodies (indicated by closed arrowheads). Protein loading was confirmed by detecting rhoptry-associated membrane antigen (RAMA), indicated by open arrowheads. The relative RON11 band intensity, measured by ImageQuant TL, was shown as Supplementary Fig. S4. (F) IFA of *Pb*RON11 in transgenic oocyst-derived sporozoites. *Pb*RON11 localisation to the apical end of sporozoites was examined by IFA using *Pb*RON11N antibodies (green (white), indicated by a closed arrowhead) and DAPI (blue). Specific signal was undetectable at the apical end (open arrowheads) of *Pb*RON11-cKD sporozoites. Differential interference contrast images are shown on the right. Scale bars = 10 μm.

homogenate, and cDNA was synthesised using a PrimeScript RT reagent Kit (Perfect Real Time, Takara). Parasite levels in the liver were examined using real-time RT-PCR to assay parasite 18S rRNA mRNA, normalised to murine *glyceraldehyde 3-phosphate dehydrogenase* (*gapdh*) mRNA. The experiment was performed with six mice in total for each parasite line and the mean and standard deviations were determined.

2.14. Sporozoite invasion assay in vitro

Ten thousand haemolymph sporozoites collected on day 21 post-feeding were inoculated onto human hepatocellular carcinoma cells, HepG2, with RPMI 1640 containing 10% FCS in eight well chamber slides (Thermo Fisher Scientific). After adding sporozoites, slides were centrifuged at 500g for 5 min at room temperature and incubated for 1 h at 37 °C with 5% CO_2. Sporozoites were fixed with 5% formalin and blocked with 5% skim milk overnight at

4 °C prior to incubation with anti-circumsporozoite protein (CSP) antibodies. The numbers of sporozoites invaded in or attached to HepG2 cells were examined by an invasion assay using two kinds of anti-CSP antibodies (Ishino et al., 2004). To distinguish between extra- and intracellular sporozoites, extracellular sporozoites were labelled with anti-rabbit CSP-repeat region antibodies, followed by Alexa Fluor 488 conjugated goat anti-rabbit IgG antibodies (1:500; Thermo Fisher Scientific). The HepG2 cells were then permeabilised with ice-cold methanol and re-labelling using anti-CSP monoclonal antibodies (MRA-100; obtained through BEI Resources, NIAID, NIH) followed by Alexa Fluor 546 conjugated goat anti-mouse IgG antibodies (1:500; Thermo Fisher Scientific). The numbers of sporozoites which had attached to or invaded cells were examined by quantification of double- or single-stained sporozoites under a fluorescence microscope (Carl Zeiss). This experiment was performed in three wells and performed in triplicate.

2.15. Sporozoite gliding motility

Haemolymph sporozoites collected on day 21 post-feeding in RPMI 1640 by perfusion were mixed with an equal volume of RPMI 1640 containing 20% FCS, and then inoculated into a glass bottom dish (Ina-optica, Osaka, Japan) and incubated for 20 min at 37 °C. Sporozoite moving patterns were observed using an AxioVert inverted fluorescence microscope (Carl Zeiss) and recorded with an AxioCam MRm Charge-Coupled Device camera (Carl Zeiss) every 2 s for up to 45 frames. Sporozoite motility patterns were categorised into: (1) drifting, (2) waving, and (3) gliding (Hegge et al., 2009). At least 100 sporozoites were observed for each line. The experiment was performed in triplicate.

2.16. TRAP discharge during sporozoites gliding

To investigate discharge of TRAP protein in sporozoites during gliding, haemolymph sporozoites collected on day 21 post-feeding were mixed with an equal volume of RPMI 1640 containing 20% FCS, transferred to eight well Permanox chamber slides, and then incubated for 30 min at 37 °C. Slides were fixed in 5% formalin for 20 min at room temperature and incubated with anti-TRAP antisera (ectodomain; 1:1,000) and ascites containing anti-CSP monoclonal antibodies (1:10,000) for 30 min at 37 °C. After washing with PBS, slides were incubated with two colours of fluorescence-conjugated secondary antibodies, Alexa Fluor 488 goat anti-rabbit IgG (1:500) and Alexa Fluor 546 goat anti-mouse IgG (1:500; Thermo Fisher Scientific), for 45 min at 37 °C. Sporozoites were categorised into four groups depending on TRAP and CSP staining patterns: (1) continuous gliding, in which TRAP was discharged to the posterior end of sporozoites and sporozoites completed more than three circles; (2) discontinuous gliding, in which TRAP was discharged to the posterior end, but gliding stopped after 1–2 circles; (3) apical pattern, in which TRAP was discharged but remained at the apical end and sporozoites could not progress through a circle; and (4) undetectable, in which TRAP could not be detected nor did sporozoites glide. At least 100 sporozoites were observed for each parasite line. The experiment was performed in triplicate.

3. Results

3.1. PbRON11 is expressed in sporozoites and localises to rhoptries

PbRON11 (PBANKA_132710) has an architecture composed of an N-terminal signal peptide, seven transmembrane domains, and two predicted Ca^{2+} binding EF-hand domains at the C-terminus (Fig. 1A). A previous accession number is listed in this manuscript since the latest annotation (PBANKA_1327100) in PlasmoDB release version 41 contains an incorrect prediction of the pbron11 exon–intron structure. RON11 is highly conserved among Plasmodium spp., as well as among other apicomplexan parasites such as the coccidians Toxoplasma gondii (TGME49_230350, Beck et al., 2013; Wang et al., 2016) and Eimeria falciformis (EfaB_PLUS_38343.g2529); the piroplasmida Theileria equi (BEWA_008660) and Babesia microti (BMR1_02g03645); and is less conserved in Cryptosporidium parvum (cgd3_2010). RON11 orthologues contain similar features of a signal peptide, multiple transmembrane domains, and two EF hand domains. The amino acid sequence similarity in the EF-hand domains suggests that a Ca^{2+}-binding capacity is important for protein function (Supplementary Fig. S3).

To characterise the expression and localisation of PbRON11, antibodies against PbRON11 were prepared by immunisation of a rabbit with recombinant protein corresponding to the N-terminal region of mature PbRON11 (PbRON11N, indicated by a bar in Fig. 1A). To evaluate the reactivity and specificity of PbRON11N antibodies, western blot analysis was performed using a PbWT-GFP schizont-enriched protein lysate. Anti-PbRON11N antibodies specifically detected a protein as a single band at approximately 100 kDa, which is consistent with the predicted size of mature PbRON11 protein (Fig. 1B, left lane). PbRON11 expression during sporozoite maturation in mosquitoes was also examined using sporozoites collected from midguts, haemolymph, and salivary glands of infected Anopheles stephensi at day 23 post-feeding. Western blot results revealed that PbRON11 was detected migrating at approximately 100 kDa in all sporozoite samples (Fig. 1B and Supplementary Fig. S4A), indicating that PbRON11 is synthesised early in sporozoite formation and the protein is present until after sporozoites invade salivary glands. This finding also suggests that PbRON11 is not cleaved during sporozoite maturation in mosquito bodies.

To examine PbRON11 localisation, IFA was performed on P. berghei schizonts and sporozoites. PbRON11 was detected as a punctate pattern in mature schizonts. PbRON11 signal was distributed somewhat widely in the anterior part of sporozoites collected from midguts, and was concentrated in the apical region of sporozoites collected from haemolymph or salivary glands (Fig. 1C). IEM was performed to refine localisation of PbRON11. PbRON11 was demonstrated to localise to the neck portion of rhoptry of merozoites (Fig. 1D). However, the signal for PbRON11 in sporozoites was not abundant by IEM using specific antibodies. Therefore, we generated transgenic parasites expressing PbRON11 fused with a c-Myc-tag at the C-terminus (PbRON11-c-Myc; Supplementary Fig. S1). PbRON11 tagged with c-Myc was confirmed to localise to the rhoptry neck region in merozoites (Supplementary Fig. S5A). PbRON11 tagged with c-Myc in sporozoites collected from salivary glands was localised to rhoptries, but not restricted to the neck portion (Fig. 1E). This tendency was also observed in PbWT-GFP sporozoites using anti-RON11N antibodies, although less signal was detected (Supplementary Fig. S5B). The specificity of anti-c-Myc antibodies was confirmed using PbWT-GFP sporozoites as a negative control (Supplementary Fig. S5C).

3.2. PbRON11 is crucial for sporozoite invasion of mosquito salivary glands

Previous attempts to disrupt the pbron11 locus were not successful, suggesting that PbRON11 is essential for asexual blood-stage parasite proliferation (Lasonder et al., 2008; van Ooij et al., 2008), the stage in which gene disruptions are performed. Therefore, to examine the function of PbRON11 in sporozoites, we applied the promoter swapping strategy by which another rhoptry protein, RON2, was successfully repressed only in sporozoites (Ishino et al., 2019). The promoter region of pbron11 was replaced by homologous recombination with a pbmsp9 promoter, which is active in schizonts but silenced in sporozoites (Fig. 2A). Two independent pbron11 conditional knockdown (PbRON11-cKD) parasite clones were obtained and named PbRON11-cKD clone 1 (cl1) and clone 2 (cl2). As a control, PbRON11 control parasites (PbRON11-cont) were generated by integration of a transfection vector at the pbron11 locus without changing the pbron11 promoter sequence (Fig. 2B).

To confirm the correct integration of the transgenic vector into the pbron11 locus, genomic Southern blot analysis was performed. A DNA probe corresponding to the hDHFR expression cassette reacted specifically to DNA fragments at approximately 5.7 kbp or 5.8 kbp in the genomic DNA of PbRON11-cont or PbRON11-cKD parasites, respectively, confirming that the pbron11 promoter region was successfully replaced by the transgenic vector (Fig. 2C). To examine whether pbron11 transcription was decreased in

PbRON11-cKD sporozoites, quantitative RT-PCR was performed using sporozoites collected from midgut oocysts of PbWT-GFP, Pb-RON11-cont, and PbRON11-cKD. It was confirmed that transcription of pbron11 in sporozoites of PbRON11-cKD cl1 and cl2 was 80 to 90 times less than that of PbWT-GFP or PbRON11-cont (Fig. 2D). PbRON11 protein expression among parasite lines (Pb-WT-GFP, PbRON11-cont, PbRON11-cKD cl1 and cl2) in schizonts and sporozoites was compared by western blot analysis. The intensity of the 100 kDa band corresponding to PbRON11 was equivalent in schizonts among four parasite lines, indicating that PbRON11 production is normal in schizonts of mutant lines (Fig. 2E, left panels and Supplementary Fig. S4B). This result agrees with the finding that PbRON11-cKD parasites proliferate equally to PbWT-GFP in the intraerythrocytic stage (Supplementary Fig. S6). In contrast, PbRON11 signal intensities in PbRON11-cKD cl1 and cl2 sporozoites collected from midgut oocysts were less than 1/20 of that in PbRON11-cont (Fig. 2E right panels and Supplementary Fig. S4C). The reduction in PbRON11 protein expression in Pb-RON11-cKD sporozoites was further confirmed by IFA. The fluorescence signals corresponding to PbRON11 were undetectable in PbRON11-cKD cl1 or cl2 sporozoites (Fig. 2F). These results indicate that the expression of PbRON11 protein in PbRON11-cKD sporozoites was reduced by at least 95% compared with that of the control parasites. In addition, the amounts of other rhoptry proteins, known to form complexes in merozoites (Cao et al, 2009), were examined in PbRON11-cKD sporozoites by western blotting (Supplementary Fig. S7). RON2 and RON4 amounts in Pb-RON11-cKD sporozoites were more than 70% of those in control sporozoites, indicating that pbron11 knockdown had no non-specific effect on sporozoite rhoptry protein levels. Taken together, these results support the use of PbRON11-cKD parasites in the following experiments to elucidate PbRON11 function in sporozoites.

In phenotypic analyses we first investigated sporozoite formation in mosquito midgut oocysts and the migration ability of Pb-RON11-cKD cl1 sporozoites. Sporozoites were collected and counted from midguts, haemolymph, and salivary glands of infected mosquitoes at day 23 post-feeding. The numbers of sporozoites from midguts of PbRON11-cKD (cl1 and cl2) infected mosquitoes were similar to those of PbRON11-cont infected

mosquitoes, indicating that sporozoite formation occurs normally in PbRON11-cKD (Fig. 3A). The number of sporozoites collected from haemolymph of PbRON11-cKD infected mosquitoes were also similar to the control, indicating that PbRON11-cKD sporozoites are released normally from oocysts into the haemocoel at a similar efficiency to PbRON11-cont (Fig. 3B). In contrast, the numbers of sporozoites collected from salivary glands of mosquitoes infected with PbRON11-cKD cl1 and cl2 were significantly reduced, by approximately 200-fold or 120-fold, respectively, compared with that of PbRON11-cont infected mosquitoes (Fig. 3C). Therefore, we concluded that the reduction in the number of sporozoites collected from salivary glands was due to the repression of the PbRON11 protein amount in sporozoites. This finding demonstrates that PbRON11 plays a crucial role for sporozoite invasion of mosquito salivary glands. Hereafter, PbRON11-cKD cl1 parasites were used for further phenotypic investigation.

3.3. PbRON11 is required for the infection of sporozoites in mammalian hosts

To investigate whether PbRON11 is also important for infection of mammalian hosts, we characterised the infectivity of sporozoites to the liver, the first target in mammalian hosts. Since it is difficult to obtain large numbers of PbRON11-cKD sporozoites from salivary glands, the following experiments were conducted using haemolymph-derived sporozoites, which are infectious to mammalian hosts when injected intravenously (Sato et al., 2014). Pb-RON11-cont or PbRON11-cKD cl1 sporozoites were intravenously injected into C57BL/6 mice and the livers, perfused with PBS, were harvested 24 h later. To compare the parasite burden in the liver, the amount of Pb18S rRNA was measured, normalised to the amount of murine gapdh mRNA. The amount of parasite 18S rRNA in the livers infected with PbRON11-cKD sporozoites was reduced by approximately 10,000-fold compared with that of livers infected with PbRON11-cont (Fig. 4A). This result clearly demonstrates that PbRON11 is important for sporozoite infectivity to the mouse liver.

Explanations for impaired PbRON11-cKD sporozoite infectivity to the mouse liver include: (i) sporozoites failed to pass through
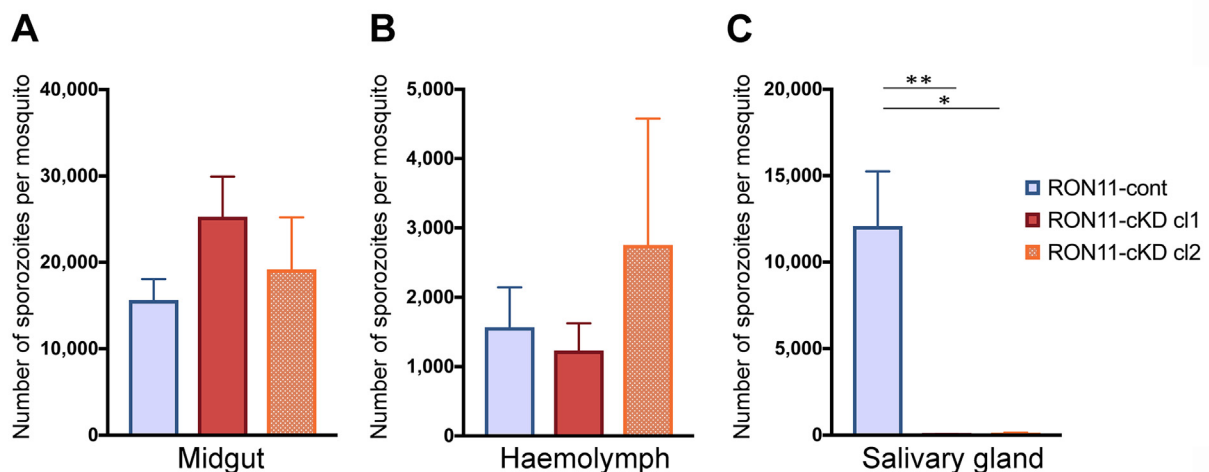
Fig. 3. Plasmodium berghei rhoptry neck protein 11 (PbRON11) is important for sporozoite invasion of salivary glands. The numbers of sporozoites collected from mosquito midguts (A), haemolymph (B), and salivary glands (C) are shown. Mosquitoes infected with PbRON11-cont (mauve (light grey)), PbRON11-cKD cl1 (red (dark grey)), or PbRON11-cKD cl2 (orange (grey with white dots)) parasites were dissected at day 23 post-feeding, and the numbers of sporozoites per mosquito were compared among parasite lines. At least 30 mosquitoes were dissected for each group and the mean numbers of sporozoites per mosquito with standard deviation from at least four independent experiments are shown as bar graphs. P-values were calculated using by the Kruskal–Wallis test with the Dunn's multiple comparisons test. No significant difference was observed in the number of sporozoites collected from midguts (A, P value: 0.2344) or from haemolymph (B, P value: 0.9914). In contrast, the number of sporozoites collected from salivary glands was significantly different (C, P value: 0.0001). The P value from post-hoc analysis is shown in the graph ($^{**}P < 0.001$; $^{*}P < 0.05$).
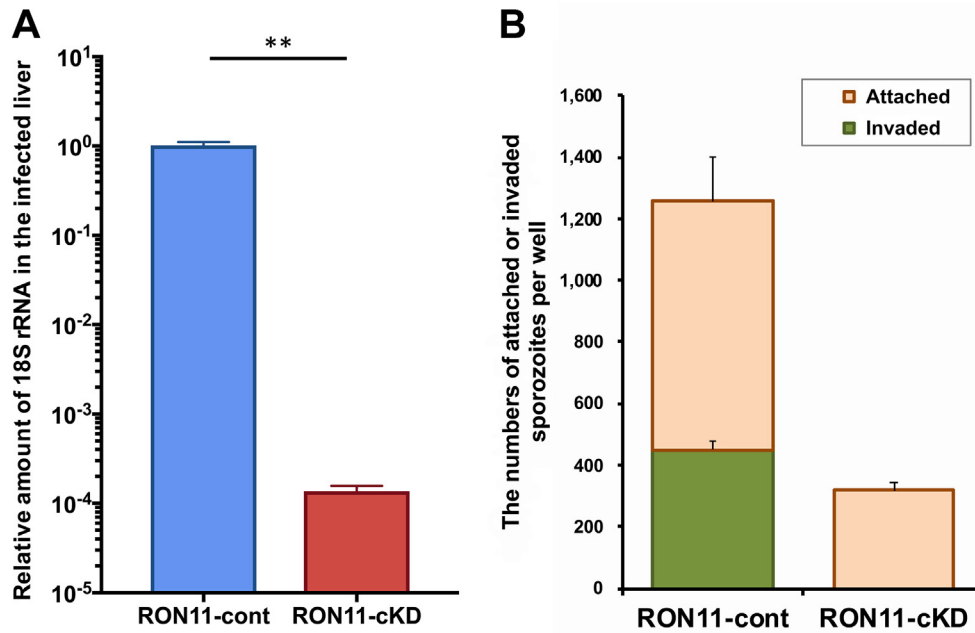
Fig. 4. *Plasmodium berghei* rhoptry neck protein 11 (*Pb*RON11) is important for sporozoite infection of the mouse liver. (A) Quantification of parasite amounts in the mouse liver at 24 h after sporozoite inoculation. Twenty thousand haemolymph sporozoites of *Pb*RON11-cont or *Pb*RON11-cKD cl1 were injected into mice intravenously (six mice per parasite line). The amount of parasite 18S rRNA in the liver at 24 h after inoculation was measured by real-time reverse transcription (RT)-PCR and normalised by the amount of murine *glyceraldehyde 3-phosphate dehydrogenase* (*gapdh*) mRNA. The average values of relative parasite 18S rRNA levels, normalised to the mouse *gapdh* mRNA level, of six mice from two independent experiments are shown with standard deviations as error bars. The statistical difference in the relative expression of Pb18S rRNA between *Pb*RON11-cont and *Pb*RON11-cKD was calculated by the Mann–Whitney *U*-test ([**]$P < 0.01$). (B) Quantification of intra- and extracellular sporozoites on HepG2 cells using fluorescence microscopy. Ten thousand haemolymph sporozoites of either *Pb*RON11-cont or *Pb*RON11-cKD cl1 were added to HepG2 cells and incubated for 1 h at 37 °C. The numbers of sporozoites which invaded (green (dark grey)) or attached to (orange (light grey)) HepG2 cells were examined by invasion assay. The mean values for three wells and standard deviations are shown in the graph. The experiments were performed in triplicate.

the sinusoidal cell layer before reaching hepatocytes, (ii) sporozoites failed to invade hepatocytes, or (iii) sporozoites could not develop in hepatocytes. To investigate whether *Pb*RON11 is essential for the invasion process into hepatocytes, an in vitro culture system was applied using human hepatoma cells, HepG2. Sporozoites isolated from haemolymph were forced to contact HepG2 cells by centrifugation after inoculation. Cells were washed and fixed with paraformaldehyde 1 h after incubation, and then intra- or extracellular sporozoites were distinguished by double staining IFA. For the *Pb*RON11-cont line, greater than 12% of the 10,000 sporozoites in the assay adhered to or invaded HepG2 cells. Approximately 35% of these sporozoites invaded intracellularly. In contrast, for the *Pb*RON11-cKD line, approximately 3.5% of the 10,000 sporozoites in the assay adhered to the surface of HepG2 cells, and no sporozoites were observed intracellularly (Fig. 4B). These findings indicate that *Pb*RON11 is required for sporozoite attachment to hepatocytes and is additionally crucial for invasion of hepatocytes.

3.4. PbRON11 is important for adhesion and gliding movement of sporozoites

Since it is known that motility is important for sporozoites to invade salivary glands and hepatocytes (Sultan et al., 1997; Combe et al., 2009; Ejigiri and Sinnis, 2009), we examined the gliding ability of haemolymph-derived *Pb*RON11-cKD sporozoites in vitro. Based on the description of Hegge et al. (2009), the movement patterns of sporozoites activated by FCS-containing medium and observed by live imaging were classified into the following three types: (1) drifting; (2) waving, with only one tip of the sporozoite attached to glass slides; and (3) gliding, typically in a circular movement on glass slides. In the *Pb*RON11-cont line, 43% of sporozoites attached to glass slides and two-thirds of them

demonstrated gliding motility. In contrast, only 7% of *Pb*RON11-cKD sporozoites could attach and no gliding sporozoites were observed (Fig. 5A). These results suggest that *Pb*RON11 is important for adhesion and gliding motility of sporozoites. The impairment of attachment and motility in *Pb*RON11-cKD sporozoites could explain the severe defect in *Pb*RON11-cKD sporozoite invasion of salivary glands and hepatocytes.

TRAP discharge to the sporozoite plasma membrane and translocation toward the posterior end has been reported to be essential for gliding motility. An increase in cytosolic Ca^{2+} levels, caused by sporozoite activation and further enhanced by attachment to the substrate, stimulates the discharge of TRAP stored in micronemes (Carey et al., 2014). Therefore, we examined the possibility that *Pb*RON11 is involved in *Pb*TRAP discharge from the microneme prior to gliding. *Pb*RON11-cont and *Pb*RON11-cKD sporozoites were collected from haemolymph and incubated in FCS-containing medium for 30 min to induce gliding motility in vitro. Discharge of *Pb*TRAP from micronemes to the surface of sporozoites was detected by staining attached sporozoites with anti-*Pb*TRAP ectodomain antibodies without permeabilisation. Gliding trails were confirmed by staining with anti-CSP antibodies. In *Pb*RON11-cont, normal gliding movement with TRAP discharge was observed in 69% of attached sporozoites. *Pb*TRAP discharge was observed in 67% of *Pb*RON11-cKD sporozoites, which is comparable to *Pb*RON11-cont, indicating that *Pb*TRAP discharge itself was not affected by *Pb*RON11 repression (Fig. 5B). However, among TRAP discharged *Pb*RON11-cKD sporozoites, 55% stopped movement after progressing less than two circles and 22% did not show any migration, in which TRAP was not transported towards the posterior end (Fig. 5B). These results suggest that RON11 could be involved in processes later than TRAP discharge. In contrast to *Pb*TRAP, no *Pb*RON11 signal was detected on the surface or the apical tip of activated control sporozoites, as visualised using
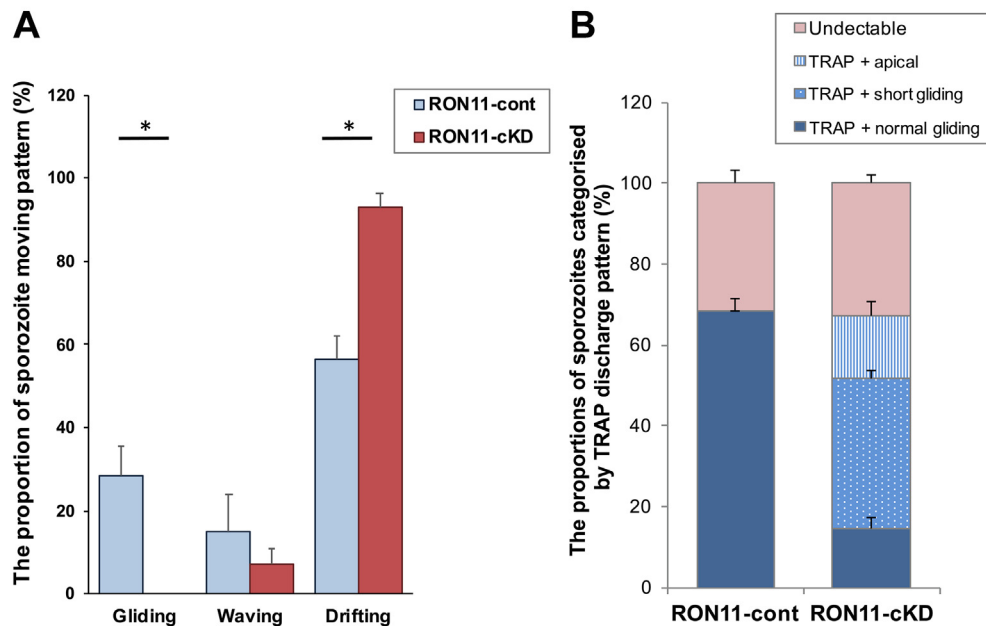
Fig. 5. *Plasmodium berghei* rhoptry neck protein 11 (*Pb*RON11) is essential for sporozoite gliding motility. (A) Gliding motility was compared between *Pb*RON11-cont and *Pb*RON11-cKD cl1 haemolymph sporozoites in vitro. Sporozoites were activated by incubation in 10% FCS-containing medium and their movement patterns were classified into three categories: gliding, waving, and drifting. At least 100 sporozoites were observed for each parasite line and the mean proportions of each moving pattern with standard deviations from three independent experiments are shown. The statistical differences in the percentages of sporozoites with each moving pattern between *Pb*RON11-cont and *Pb*RON11-cKD were calculated by the Mann–Whitney *U*-test ($^*P < 0.05$). (B) *Pb*RON11 is dispensable for *Pb* thrombospondin-related adhesive protein (TRAP) discharge from micronemes. Haemolymph sporozoites were incubated in activation medium for 30 min, fixed by formalin, and double stained by antibodies against the *Pb*TRAP ectodomain and *Pb* circumsporozoite protein (CSP). At least 100 sporozoites were observed and classified into four categories: continuous gliding, in which TRAP was discharged to the posterior end and released as a trail during sporozoite gliding (TRAP + normal gliding, blue (dark grey)); discontinuous gliding, in which TRAP was discharged and released as a trail, but gliding stopped after 1–2 circles (TRAP + short gliding, light blue (medium grey) with dotted pattern); apical pattern, in which TRAP was discharged but remained at the apical end of sporozoites which could not progress through a circle (TRAP + apical, pale blue (light grey) with stripe pattern); and undetectable, in which TRAP could not be detected nor did sporozoites glide (Undetectable, pink (light grey)). Each bar represents the mean values with standard deviations from three independent experiments.

anti-*Pb*RON11N antibodies (Supplementary Fig. S8), indicating that *Pb*RON11 remains inside the rhoptries during gliding.

4. Discussion

RON11 is a molecule predicted to possess multiple transmembrane regions and two EF-hand domains that bind Ca^{2+}. Structural analysis of *Pb*RON11 using the protein modelling module of Phyre2 (Kelley et al., 2015) revealed that the conformation of 786–944 amino acid of *Pb*RON11 showed high homology with that of known proteins having an EF-hand domain pair. Therefore, RON11 is likely to have Ca^{2+} binding ability (Lewit-Bentley and Rety, 2000). Eight amino acid residues implicated in Ca^{2+} binding are conserved across *Plasmodium*, and seven amino acids are conserved between *Toxoplasma* and *Plasmodium* (Supplementary Fig. S3). The multiple transmembrane region of RON11 is also well conserved among apicomplexan orthologues, suggesting that it is similarly important for the function of RON11. A possible RON11 orthologue (Vbra_11269) is encoded in the genome of the alveolate *Vitrella brasillica*, a free-living non-parasitic photosynthetic alga closely related to apicomplexans. This suggests that RON11 originated prior to the specialisation to obligate parasitism in the Apicomplexa, perhaps involved in secretion in alveolate rhoptry-like organelles. The N-terminal region of RON11 possesses a predicted erythrocyte cytoplasm-targeting PEXEL motif, which is conserved in all *Plasmodium* but not in *Toxoplasma* orthologues. The function of this motif is unknown since RON11 is targeted to the rhoptries of merozoites and sporozoites. The majority of PEXEL-containing proteins are encoded by genes having a 2-exon structure, and thus the numerous exons of *ron11* depart from the canonical gene structure. We failed to detect exported RON11 in the cytoplasm of infected erythrocytes using anti-RON11N antibodies. A role for the PEXEL motif in rhoptry-targeted RON11, or an alternative trafficking pathway directing RON11 to the erythrocyte cytoplasm, awaits further inquiry.

In the Apicomplexa, the control of intracellular Ca^{2+} concentration has been reported to be important in motility and invasion (Billker et al., 2009; Kebaier and Vanderberg, 2010; Singh et al., 2010). It is known that elevated calcium levels in the cytoplasm promotes secretion from micronemes, putting in motion the machinery driving motility and invasion (Carruthers and Sibley, 1999); and a subsequent drop in calcium concentration is associated with rhoptry protein secretion (Singh et al., 2010). Pharmacological analysis has predicted an inositol triphosphate receptor (IP3R) to be involved in the release of Ca^{2+} stored in the cytoplasm of malaria parasites (Beraldo et al., 2007; Alves et al., 2011). However, no IP3R orthologous have been found in the complete genomes of multiple *Plasmodium* spp. Phosphoinositide phospholipase C (PI-PLC) is present in malaria parasites (Raabe et al., 2011), and its specific inhibitor has been shown to suppress the motility of sporozoites (Carey et al., 2014), but the G-protein coupled receptor on the cytoplasmic membrane to which PI-PLC binds remains unknown. In mammals, polycystin-2 and ryanodine receptors possess EF-hand domains plus multiple transmembrane domains, and it has been reported that they exhibit Ca^{2+} channel activity in a Ca^{2+} concentration-dependent manner (Lai and Meissner, 1989; Petri et al., 2010). It is of interest to determine if RON11 exhibits channel activities, as well as to characterise its protein binding partners.

We believe this is the first report describing the localisation of RON11 by electron microscopy in *Plasmodium* merozoites and sporozoites. In merozoites, *Pb*RON11 was confined to the rhoptry neck region, whereas in sporozoites *Pb*RON11 was found with a broader localisation inside the rhoptries. The subcellular localisation of *Pb*RON2 and *Pb*RON12 similarly varies in merozoites and sporozoites (Ishino et al., 2019; Oda-Yokouchi et al., 2019), and thus may reflect a difference in the function or mode of action of merozoite versus sporozoite expression of RON proteins. When sporozoites were activated in vitro to induce gliding motility on glass slides, *Pb*RON11 was never observed released from rhoptries to the apical tip or the surface of sporozoites (Supplementary Fig. S8), in contrast to the surface translocation of TRAP (Menard, 2001). Therefore, RON11 may function inside rhoptries in a Ca^{2+}-dependent manner, such as controlling the secretion of other rhoptry proteins involved in the invasion of both mosquito salivary glands and mammalian hepatocytes.

In *Plasmodium*, RON11 is believed to be essential for parasite proliferation in the intraerythrocytic asexual stage, due to an inability to disrupt the *ron11* gene (Lasonder et al., 2008; van Ooij et al., 2008). In contrast, in *Toxoplasma* tachyzoites it was demonstrated that RON11 is dispensable for invasion (Wang et al., 2016). In this study, by applying a sporozoite stage-specific knockdown system (Ishino et al., 2019), RON11 protein expression in sporozoites was repressed to 1/20 or less of the control, which enabled us to analyse the function(s) of RON11 in sporozoites. First, *Pb*RON11 was shown to be important for salivary gland invasion, whereas it is dispensable for sporozoite formation and release to the haemocoel. Next it was revealed, in vivo and in vitro, that *Pb*RON11 plays an important role in hepatocyte invasion. Using the same knockdown system, we have revealed that *Pb*RON2 is also important for sporozoite invasion of salivary glands and mammalian hepatocytes; however, the RON2 involvement for invasion of hepatocytes is smaller (Ishino et al., 2019). As *Pb*RON11-cKD sporozoites showed stronger phenotypes in motility and invasive ability to hepatocytes, it would be interesting to investigate whether RON2 and RON11 interact physically or functionally. We demonstrated that *pbron11* knockdown has a negligible impact on the RON2 protein amount, but its localisation in sporozoites needs to be investigated. These phenotypes of *Pb*RON11-cKD sporozoites are similar to those of *Pb*TRAP-disrupted sporozoites (Sultan et al., 1997; Ejigiri et al., 2012). Sporozoite invasion of salivary glands has been demonstrated to require several proteins released from micronemes such as TRAP, TRAP-related protein (TREP)/S6/UOS3 (Combe et al., 2009; Mikolajczak et al., 2008; Steinbuechel and Matuschewski, 2009), sporozoite invasion association protein-1 (SIAP-1, Engelmann et al., 2009), LIMP (Santos et al., 2017), and MAEBL (Kariu et al, 2002; Saenz et al., 2008). Our findings that the rhoptry proteins RON2 and RON11 are involved in sporozoite attachment and motility indicate that the cooperative action of molecules secreted to the tip of sporozoite from two major apical organelles, micronemes and rhoptries, could be required for the sporozoite movement and subsequent invasion mechanisms.

When sporozoites are activated by stimulation, TRAP is discharged from micronemes, dependent on the increase in the Ca^{2+} concentration in the cytoplasm, which is an essential step for gliding (Kebaier and Vanderberg, 2010). Our finding that the discharge of TRAP to the tip of activated *Pb*RON11-cKD sporozoites occurred normally suggests that *Pb*RON11 is dispensable for TRAP discharge and for an initial increase in the Ca^{2+} level in the cytoplasm. In *Pb*RON11-cKD sporozoites, however, TRAP translocation from the apical tip to the posterior end via the plasma membrane was suppressed (Fig. 5B). This observation in *Pb*RON11-cKD sporozoites is similar to that of sporozoites that are artificially increased in intracellular Ca^{2+} concentration by adding calcium ionophore (Carey et al., 2014). Taking the pharmacological analysis results together with phenotypic observations, there could be several possible explanations for the phenomenon in *Pb*RON11-cKD sporozoites. Specifically, (i) there is no further increase in Ca^{2+} concentration, as these sporozoites show low attachment ability, therefore a sufficient intracellular Ca^{2+} concentration cannot be maintained; (ii) there is no oscillation of Ca^{2+} accompanying gliding motility; (iii) events other than TRAP discharge, such as activation of the actomyosin system, binding specific to TRAP, or activation of a protease cleaving TRAP, has not occurred; and (iv) second messengers other than Ca^{2+} (such as cAMP or cGMP) do not function properly (Kebaier and Vanderberg, 2010). By detecting fluctuation of the intracellular Ca^{2+} concentration in *Pb*RON11-cKD sporozoites, better understanding of signalling pathways in the sporozoites after activation could be obtained.

Appendix A. Supplementary data

Supplementary data to this article can be found online at https://doi.org/10.1016/j.ijpara.2019.05.001.

References

Acharya, P., Kumar, R., Tatu, U., 2007. Chaperoning a cellular upheaval in malaria: heat shock proteins in *Plasmodium falciparum*. Mol. Biochem. Parasitol. 153, 85–94.

Alves, E., Bartlett, P.J., Garcia, C.R., Thomas, A.P., 2011. Melatonin and IP3-induced Ca^{2+} release from intracellular stores in the malaria parasite *Plasmodium falciparum* within infected red blood cells. J. Biol. Chem. 286, 5905–5912.

Aly, A.S., Vaughan, A.M., Kappe, S.H., 2009. Malaria parasite development in the mosquito and infection of the mammalian host. Annu. Rev. Microbiol. 63, 195–221.

Beck, J.R., Fung, C., Straub, K.W., Coppens, I., Vashisht, A.A., Wohlschlegel, J.A., Bradley, P.J., 2013. A *Toxoplasma* palmitoyl acyl transferase and the palmitoylated armadillo repeat protein TgARO govern apical rhoptry tethering and reveal a critical role for the rhoptries in host cell invasion but not egress. PLoS Pathog. 9, e1003162.

Beraldo, F.H., Mikoshiba, K., Garcia, C.R., 2007. Human malarial parasite, *Plasmodium falciparum*, displays capacitative calcium entry: 2-aminoethyl diphenylborinate blocks the signal transduction pathway of melatonin action on the *P. falciparum* cell cycle. J. Pineal Res. 43, 360–364.

Besteiro, S., Michelin, A., Poncet, J., Dubremetz, J.F., Lebrun, M., 2009. Export of a *Toxoplasma gondii* rhoptry neck protein complex at the host cell membrane to form the moving junction during invasion. PLoS Pathog. 5, e1000309.

Billker, O., Lourido, S., Sibley, L.D., 2009. Calcium-dependent signaling and kinases in apicomplexan parasites. Cell Host Microbe 5, 612–622.

Bradley, P.J., Sibley, L.D., 2007. Rhoptries: an arsenal of secreted virulence factors. Curr. Opin. Microbiol. 10, 582–587.

Cao, J., Kaneko, O., Thongkukiatkul, A., Tachibana, M., Otsuki, H., Gao, Q., Tsuboi, T., Torii, M., 2009. Rhoptry neck protein RON2 forms a complex with microneme protein AMA1 in *Plasmodium falciparum* merozoites. Parasitol. Int. 58, 29–35.

Carey, A.F., Singer, M., Bargieri, D., Thiberge, S., Frischknecht, F., Menard, R., Amino, R., 2014. Calcium dynamics of *Plasmodium berghei* sporozoite motility. Cell. Microbiol. 16, 768–783.

Carruthers, V.B., Sibley, L.D., 1999. Mobilization of intracellular calcium stimulates microneme discharge in *Toxoplasma gondii*. Mol. Microbiol. 31, 421–428.

Combe, A., Moreira, C., Ackerman, S., Thiberge, S., Templeton, T.J., Menard, R., 2009. TREP, a novel protein necessary for gliding motility of the malaria sporozoite. Int. J. Parasitol. 39, 489–496.

Ejigiri, I., Ragheb, D.R., Pino, P., Coppi, A., Bennett, B.L., Soldati-Favre, D., Sinnis, P., 2012. Shedding of TRAP by a rhomboid protease from the malaria sporozoite surface is essential for gliding motility and sporozoite infectivity. PLoS Pathog. 8, e1002725.

Ejigiri, I., Sinnis, P., 2009. *Plasmodium* sporozoite-host interactions from the dermis to the hepatocyte. Curr. Opin. Microbiol. 12, 401–407.

Engelmann, S., Silvie, O., Matuschewski, K., 2009. Disruption of *Plasmodium* sporozoite transmission by depletion of sporozoite invasion-associated protein 1. Eukaryot. Cell 8, 640–648.

Franke-Fayard, B., Trueman, H., Ramesar, J., Mendoza, J., van der Keur, M., van der Linden, R., Sinden, R.E., Waters, A.P., Janse, C.J., 2004. A *Plasmodium berghei* reference line that constitutively expresses GFP at a high level throughout the complete life cycle. Mol. Biochem. Parasitol. 137, 23–33.

Ghosh, A.K., Devenport, M., Jethwaney, D., Kalume, D.E., Pandey, A., Anderson, V.E., Sultan, A.A., Kumar, N., Jacobs-Lorena, M., 2009. Malaria parasite invasion of the mosquito salivary gland requires interaction between the *Plasmodium* TRAP and the *Anopheles* saglin proteins. PLoS Pathog. 5, e1000265.

Hegge, S., Kudryashev, M., Smith, A., Frischknecht, F., 2009. Automated classification of *Plasmodium* sporozoite movement patterns reveals a shift towards productive motility during salivary gland infection. Biotechnol. J. 4, 903–913.

Ishino, T., Yano, K., Chinzei, Y., Yuda, M., 2004. Cell-passage activity is required for the malarial parasite to cross the liver sinusoidal cell layer. PLoS Biol. 2, E4.

Ishino, T., Murata, E., Tokunaga, N., Baba, M., Tachibana, M., Thongkukiatkul, A., Tsuboi, T., Torii, M., 2019. Rhoptry neck protein 2 expressed in *Plasmodium* sporozoites plays a crucial role during invasion of mosquito salivary glands. Cell. Microbiol. 21, e12964.

Janse, C.J., Ramesar, J., Waters, A.P., 2006. High-efficiency transfection and drug selection of genetically transformed blood stages of the rodent malaria parasite *Plasmodium berghei*. Nat. Protoc. 1, 346–356.

Kappe, S., Bruderer, T., Gantt, S., Fujioka, H., Nussenzweig, V., Menard, R., 1999. Conservation of a gliding motility and cell invasion machinery in Apicomplexan parasites. J Cell Biol. 147, 937–944.

Kariu, T., Yuda, M., Yano, K., Chinzei, Y., 200. MAEBL is essential for malarial sporozoite infection of the mosquito salivary gland. J. Exp. Med. 195, 1317–1323.

Kebaier, C., Vanderberg, J.P., 2010. Initiation of *Plasmodium* sporozoite motility by albumin is associated with induction of intracellular signalling. Int. J. Parasitol. 40, 25–33.

Kelley, L.A., Mezulis, S., Yates, C.M., Wass, M.N., Sternberg, M.J., 2015. The Phyre2 web portal for protein modeling, prediction and analysis. Nat. Protoc. 10, 845–858.

Kennedy, M., Fishbaugher, M.E., Vaughan, A.M., Patrapuvich, R., Boonhok, R., Yimamnuaychok, N., Rezakhani, N., Metzger, P., Ponpuak, M., Sattabongkot, J., Kappe, S.H., Hume, J.C., Lindner, S.E., 2012. A rapid and scalable density gradient purification method for *Plasmodium* sporozoites. Malar. J. 11, 421.

Lai, F.A., Meissner, G., 1989. The muscle ryanodine receptor and its intrinsic Ca^{2+} channel activity. J. Bioenerg. Biomembr. 21, 227–246.

Lasonder, E., Janse, C.J., van Gemert, G.J., Mair, G.R., Vermunt, A.M., Douradinha, B.G., van Noort, V., Huynen, M.A., Luty, A.J., Kroeze, H., Khan, S.M., Sauerwein, R.W., Waters, A.P., Mann, M., Stunnenberg, H.G., 2008. Proteomic profiling of *Plasmodium* sporozoite maturation identifies new proteins essential for parasite development and infectivity. PLoS Pathog. 4, e1000195.

Lewit-Bentley, A., Rety, S., 2000. EF-hand calcium-binding proteins. Curr. Opin. Struct. Biol. 10, 637–643.

Matuschewski, K., Nunes, A.C., Nussenzweig, V., Menard, R., 2002. Plasmodium sporozoite invasion into insect and mammalian cells is directed by the same dual binding system. EMBO J. 21, 1597–1606.

Menard, R., 2001. Gliding motility and cell invasion by Apicomplexa: insights from the *Plasmodium* sporozoite. Cell. Microbiol. 3, 63–73.

Mikolajczak, S.A., Silva-Rivera, H., Peng, X., Tarun, A.S., Camargo, N., Jacobs-Lorena, V., Daly, T.M., Bergman, L.W., de la Vega, P., Williams, J., Aly, A.S., Kappe, S.H., 2008. Distinct malaria parasite sporozoites reveal transcriptional changes that cause differential tissue infection competence in the mosquito vector and mammalian host. Mol. Cell. Biol. 28, 6196–6207.

Oda-Yokouchi, Y., Tachibana, M., Iriko, H., Torii, M., Ishino, T., Tsuboi, T., 2019. *Plasmodium* RON12 localizes to the rhoptry body in sporozoites. Parasitol. Int. 68, 17–23.

Petri, E.T., Celic, A., Kennedy, S.D., Ehrlich, B.E., Boggon, T.J., Hodsdon, M.E., 2010. Structure of the EF-hand domain of polycystin-2 suggests a mechanism for Ca^{2+}-dependent regulation of polycystin-2 channel activity. Proc. Natl. Acad. Sci. U. S. A. 2 (107), 9176–9181.

Pfaffl, M.W., 2001. A new mathematical model for relative quantification in real-time RT-PCR. Nucleic Acids Res. 29, e45.

Proellocks, N.I., Coppel, R.L., Waller, K.L., 2010. Dissecting the apicomplexan rhoptry neck proteins. Trends Parasitol. 26, 297–304.

Raabe, A.C., Wengelnik, K., Billker, O., Vial, H.J., 2011. Multiple roles for *Plasmodium berghei* phosphoinositide-specific phospholipase C in regulating gametocyte activation and differentiation. Cell. Microbiol. 13, 955–966.

Saenz, F.E., Balu, B., Smith, J., Mendonca, S.R., Adams, J.H., 2008. The transmembrane isoform of *Plasmodium falciparum* MAEBL is essential for the invasion of *Anopheles* salivary glands. PLoS One 3, e2287.

Santos, J.M., Egarter, S., Zuzarte-Luís, V., Kumar, H., Moreau, C.A., Kehrer, J., Mair, G. R., 2017. Malaria parasite LIMP protein regulates sporozoite gliding motility and infectivity in mosquito and mammalian hosts. Elife 6, e24109.

Sato, Y., Montagna, G.N., Matuschewski, K., 2014. *Plasmodium berghei* sporozoites acquire virulence and immunogenicity during mosquito hemocoel transit. Infect. Immun. 82, 1164–1172.

Schneider, C.A., Rasband, W.S., Eliceiri, K.W., 2012. NIH Image to ImageJ: 25 years of image analysis. Nat. Methods 9, 671–675.

Shonhai, A., Boshoff, A., Blatch, G.L., 2007. The structural and functional diversity of Hsp70 proteins from *Plasmodium falciparum*. Protein Sci. 16, 1803–1818.

Sibley, C.H., Guerin, P.J., Ringwald, P., 2010. Monitoring antimalarial resistance: launching a cooperative effort. Trends Parasitol. 26, 221–224.

Sinden, R.E., Butcher, G.A., Beetsma, A.L., 2002. Maintenance of the *Plasmodium berghei* life cycle. Methods Mol. Med. 72, 25–40.

Singh, S., Alam, M.M., Pal-Bhowmick, I., Brzostowski, J.A., Chitnis, C.E., 2010. Distinct external signals trigger sequential release of apical organelles during erythrocyte invasion by malaria parasites. PLoS Pathog. 6, e1000746.

Steinbuechel, M., Matuschewski, K., 2009. Role for the *Plasmodium* sporozoite-specific transmembrane protein S6 in parasite motility and efficient malaria transmission. Cell. Microbiol. 11, 279–288.

Sultan, A.A., Thathy, V., Frevert, U., Robson, K.J., Crisanti, A., Nussenzweig, V., Nussenzweig, R.S., Menard, R., 1997. TRAP is necessary for gliding motility and infectivity of *Plasmodium* sporozoites. Cell 90, 511–522.

Topolska, A.E., Black, C.G., Coppel, R.L., 2004. Identification and characterisation of RAMA homologues in rodent, simian and human malaria species. Mol. Biochem. Parasitol. 138, 237–241.

Tsuboi, T., Takeo, S., Iriko, H., Jin, L., Tsuchimochi, M., Matsuda, S., Han, E.T., Otsuki, H., Kaneko, O., Sattabongkot, J., Udomsangpetch, R., Sawasaki, T., Torii, M., Endo, Y., 2008. Wheat germ cell-free system-based production of malaria proteins for discovery of novel vaccine candidates. Infect. Immun. 76, 1702–1708.

van Ooij, C., Tamez, P., Bhattacharjee, S., Hiller, N.L., Harrison, T., Liolios, K., Kooij, T., Ramesar, J., Balu, B., Adams, J., Waters, A.P., Janse, C.J., Haldar, K., 2008. The malaria secretome: from algorithms to essential function in blood stage infection. PLoS Pathog. 4, e1000084.

Vanderberg, J.P., Frevert, U., 2004. Intravital microscopy demonstrating antibody-mediated immobilisation of *Plasmodium berghei* sporozoites injected into skin by mosquitoes. Int. J. Parasitol. 34, 991–996.

Wang, K., Peng, E.D., Huang, A.S., Xia, D., Vermont, S.J., Lentini, G., Lebrun, M., Wastling, J.M., Bradley, P.J., 2016. Identification of Novel O-Linked Glycosylated *Toxoplasma* Proteins by Vicia villosa Lectin Chromatography. PLoS One 11, e0150561.

Yang, A.S.P., Lopaticki, S., O'Neill, M.T., Erickson, S.M., Douglas, D.N., Kneteman, N. M., Boddey, J.A., 2017. AMA1 and MAEBL are important for *Plasmodium falciparum* sporozoite infection of the liver. Cell. Microbiol. 19, e12745.